Potent cross-reactive neutralization of SARS coronavirus isolates by human monoclonal antibodies

Zhongyu Zhu*†, Samitabh Chakraborti†, Yuxian He‡, Anjeanette Roberts§, Tim Sheahan¶, Xiaodong Xiao*, Lisa E. Hensley‖, Ponraj Prabakaran*, Barry Rockx¶, Igor A. Sidorov*, Davide Corti**, Leatrice Vogel§, Yang Feng*, Jae-Ouk Kim††, Lin-Fa Wang‡‡, Ralph Baric¶, Antonio Lanzavecchia**, Kristopher M. Curtis‖, Gary J. Nabel††, Kanta Subbarao§, Shibo Jiang‡, and Dimiter S. Dimitrov*§§

*Protein Interactions Group, Center for Cancer Research Nanobiology Program, and †Basic Research Program, SAIC-Frederick, Inc., National Cancer Institute-Frederick, National Institutes of Health, Frederick, MD 21702; ‡Laboratory of Viral Immunology, Lindsley F. Kimball Research Institute, New York Blood Center, New York, NY 10021; §Laboratory of Infectious Diseases and ††Vaccine Research Center, National Institute of Allergy and Infectious Diseases, National Institutes of Health, Bethesda, MD 20892; ¶Department of Epidemiology, University of North Carolina, Chapel Hill, NC 27599; ‖Virology Division, United States Army Medical Research Institute of Infectious Diseases, Fort Detrick, MD 21702; **Institute for Research in Biomedicine, Via Vela 6, CH 6500 Belllinzona, Switzerland; and ‡‡CSIRO Livestock Industries, Australian Animal Health Laboratory and Australian Biosecurity Cooperative Research Center for Emerging Infectious Diseases, Geelong, Victoria 3220, Australia

Edited by Bernard Roizman, University of Chicago, Chicago, IL, and approved May 3, 2007 (received for review February 7, 2007)

The severe acute respiratory syndrome coronavirus (SARS-CoV) caused a worldwide epidemic in late 2002/early 2003 and a second outbreak in the winter of 2003/2004 by an independent animal-to-human transmission. The GD03 strain, which was isolated from an index patient of the second outbreak, was reported to resist neutralization by the human monoclonal antibodies (hmAbs) 80R and S3.1, which can potently neutralize isolates from the first outbreak. Here we report that two hmAbs, m396 and S230.15, potently neutralized GD03 and representative isolates from the first SARS outbreak (Urbani, Tor2) and from palm civets (SZ3, SZ16). These antibodies also protected mice challenged with the Urbani or recombinant viruses bearing the GD03 and SZ16 spike (S) glycoproteins. Both antibodies competed with the SARS-CoV receptor, ACE2, for binding to the receptor-binding domain (RBD), suggesting a mechanism of neutralization that involves interference with the SARS-CoV–ACE2 interaction. Two putative hot-spot residues in the RBD (Ile-489 and Tyr-491) were identified within the SARS-CoV spike that likely contribute to most of the m396-binding energy. Residues Ile-489 and Tyr-491 are highly conserved within the SARS-CoV spike, indicating a possible mechanism of the m396 cross-reactivity. Sequence analysis and mutagenesis data show that m396 might neutralize all zoonotic and epidemic SARS-CoV isolates with known sequences, except strains derived from bats. These antibodies exhibit cross-reactivity against isolates from the two SARS outbreaks and palm civets and could have potential applications for diagnosis, prophylaxis, and treatment of SARS-CoV infections.

epitope | paratope | vaccine | therapeutic

The severe acute respiratory syndrome coronavirus (SARS-CoV) (1–4) caused a worldwide epidemic in 2002 and 2003 and infected >8,000 humans with a fatality rate of ≈10%. It reemerged in the winter of 2003/2004 when four individuals were infected by an independent transmission from palm civets (5–8). Although there has not been a natural human outbreak since 2003/2004, the need to develop potent therapeutics and vaccines against a re-emerging SARS-CoV remains of high importance because SARS-CoV or a related virus may be reintroduced into the human population from an animal reservoir or accidentally released from a laboratory. SARS-CoV infection leads to generation of potent neutralizing Abs (nAbs). Antibodies that neutralize the virus *in vitro* were also detected in SARS-CoV-infected patients (9–14) and in mice (15), hamsters (16), and monkeys (17) infected with the virus. By passive transfer of immune serum before intranasal challenge, these antibodies also protected naïve animals from SARS-CoV infection in a mouse model of SARS-CoV replication (15). Several groups have recently developed human monoclonal Abs (hmAbs) to the SARS-CoV spike (S) glycoprotein that neutralize the virus and have potential for therapy and prophylaxis of SARS (18–26; for review see ref. 23). However, data demonstrating activities of any of the identified hmAbs against isolates from the second SARS outbreak and isolates of closely related viruses isolated from animals have yet to be published. Recently, it was found that the GD03 strain, isolated from the first patient of the second (2003/2004) outbreak, is resistant to neutralization by two of the previously characterized hmAbs, 80R and S3.1 (18–20, 27).

We have previously identified fragments containing the receptor-binding domain (RBD), which is a major SARS-CoV neutralization determinant (23, 28–33), and residues critical for its binding to ACE2 (34, 35). One of these fragments containing residues 317–518 was cloned into a baculovirus expression vector, expressed in insect cells, and purified. This fragment was used as a selecting antigen for panning of a large ($\approx 10^{10}$ different antibodies) human antibody Fab library that we constructed from the B lymphocytes of healthy volunteers. An antibody, m396, was identified and crystallized in complex with the RBD, and the structure of the complex was determined at high (2.3 Å) resolution (36); we also isolated another antibody, S230.15, from immortalized B cells from a recovered SARS patient by using a previously developed methodology (18). An analysis of the structure suggested that m396 could neutralize isolates from both SARS outbreaks. Here we present evidence that these antibodies have broadly neutralizing activity against isolates from the first and second SARS outbreaks as well as from palm civets *in vitro* and in an animal model. These antibodies could be useful for prophylaxis of SARS and treatment of SARS-CoV-infected patients and as reagents to facilitate development of therapeutics and vaccines and to help understand their mechanisms of action.

Author contributions: S.C., Y.H., A.R., T.S., and X.X. contributed equally to this work; Z.Z., S.C., Y.H., A.R., T.S., X.X., L.E.H., P.P., B.R., D.C., L.V., Y.F., J.-O.K., L.-F.W., R.B., A.L., K.M.C., G.J.N., K.S., and S.J. performed research; I.A.S. analyzed data; and D.S.D. wrote the paper.

The authors declare no conflict of interest.

This article is a PNAS Direct Submission.

Abbreviations: hmAb, human monoclonal antibody; nAb, neutralizing antibody; RBD, receptor-binding domain; SARS-CoV, severe acute respiratory syndrome coronavirus; S glycoprotein, spike glycoprotein; $TCID_{50}$, tissue culture 50% infective dose.

§§To whom correspondence should be addressed at: Protein Interactions, Center for Cancer Research Nanobiology Program, National Cancer Institute, National Institutes of Health, P.O. Box B, Building 469, Room 150B, Frederick, MD 21702-1201. E-mail: dimitrov@ncifcrf.gov.

This article contains supporting information online at www.pnas.org/cgi/content/full/0701000104/DC1.

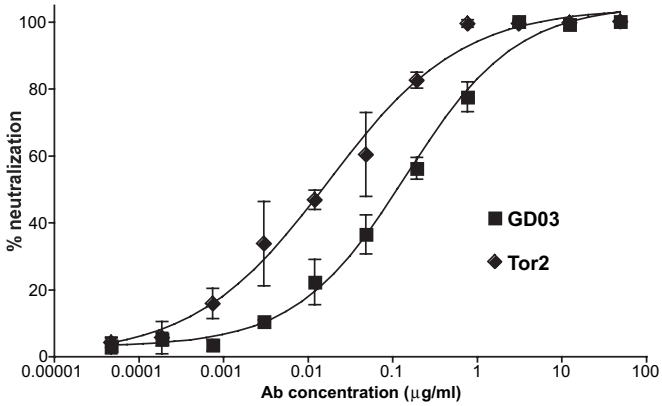

Fig. 1. M396 potently neutralizes viruses pseudotyped with S glycoproteins from the Tor2 and GD03 isolates. HIVs pseudotyped with the S glycoprotein from Tor2 and GD03 isolates were incubated with IgG1 m396 for 1 h before infection. Luciferase activities in target cells were measured, and the percent neutralization was calculated. All experiments were performed in duplicate or triplicate, and two experiments in different days were performed with essentially identical results. Bars indicate SE.

Results

Potent *in Vitro* Inhibition of Entry and Cell Fusion Mediated by the S Glycoprotein of SARS-CoV Isolates from the 2002/2003 and 2003/2004 Outbreaks and from Palm Civets. We have recently identified an hmAb, m396, which binds with high affinity to the RBD, and we determined the crystal structure of the RBD·m396 complex at high resolution (36). A crystal structure analysis suggested that this antibody could also neutralize the 2003/2004 outbreak isolate GD03. To test the inhibitory activity of m396 against GD03 and compare it with that against representative isolates from the first outbreak, we used viruses pseudotyped with the S glycoprotein of GD03 and Tor2, an isolate from the 2002/2003 outbreak. IgG1 m396 potently neutralized both GD03 and Tor2 viruses with an IC_{50} of 0.1 and 0.01 μg/ml, respectively (Fig. 1), as well as a virus pseudotyped with the S glycoprotein from the Urbani isolate (Table 1). M396 also potently neutralized infectious replication-competent viruses, Urbani and Tor2 isolates, with an IC_{50} of 0.05 and 0.06 μg/ml, respectively (Fig. 2). When tested with another live SARS-CoV isolate, HKU39849, in Vero E6 cells, 100% inhibition of infection was achieved at a concentration of 0.6 μg/ml. Another hmAb, S230.15, which we identified by using a methodology based on EBV transformation of B cells from a convalescent patient (18), also potently neutralized Urbani and Tor2 isolates (Table 1). Both antibodies neutralized the pseudotyped viruses bearing spikes from palm civet isolates SZ3 and SZ16 although with somewhat lower potency *in vitro* (Table 1). The neutralizing activity of the antibodies was similar for virus that infects cells transfected with human or palm civet ACE2 (data not shown and Table 1). Neither of the two antibodies caused enhancement of virus entry for any isolate tested (data not shown and Table 1). The two antibodies also potently neutralized recombinant replication-competent SARS-CoV isolates Urbani, GD03, and SZ16 (containing the K479N mutation to facilitate binding to human ACE2) (Table 1). M396 potently inhibited S-mediated fusion with an IC_{50} of 0.6 μg/ml [supporting information (SI) Fig. 7*A* and Table 1]. Under the same experimental conditions, another SARS-CoV-neutralizing antibody, IgG1 80R (19), exhibited an IC_{50} of 1.1 μg/ml. A control antibody that potently neutralizes Hendra and Nipah viruses did not show any inhibitory effect in this assay. These data suggest that both m396 and S230.15 exhibit potent inhibitory activity against isolates from the 2002/2003 and the 2003/2004 outbreaks as well as against isolates from palm civets.

Table 1. Comparison of the *in vitro* neutralizing activity of m396 and S215.15 with that of known SARS-CoV-neutralizing hmAbs

Antibody	Assay	Isolate	Activity
m396	Pseudovirus	Tor2	0.01
		Urbani	<1
		GD03	0.1
		SZ3	1
		SZ16	2
	Cell fusion	Tor2	0.6
	Live virus	Tor2	0.06
		HKU39849	0.6*
		Urbani	0.05
		Urbani	0.6
		GD03	1.7
	Recombinant replication-competent virus	SZ16-K479N	3.4
S230.15	Pseudovirus	Urbani	0.07
		Tor2	<1*
		SZ3	<1
		SZ16	<1
		Urbani	<0.2
		GD03	0.3
	Recombinant replication-competent virus	SZ16-K479N	0.2
S3.1	Cytopathicity	Urbani	<0.3*
	Pseudovirus	GD03	>10
		Urbani	<1
CR3014	Cytopathicity	HKU39849	<7*
		FM-1	<5*
80R	Pseudovirus	Tor2	<2
		GD03	>50
	Syncytia	Urbani	<4
	Cytopathicity	Urbani	0.06
	Cell fusion	Tor2	1.1
201	Cytopathicity	Urbani	0.2
scFv B1	Pseudovirus	Not reported	4

The data for m396, S230.15, and inhibition of cell fusion by 80R are described in this work; for S3.1, see refs. 18 and 27; for CR3014, see ref. 21; for 80R, see refs. 19 and 20; for 201, see ref. 24; and for scFv B1, see ref. 22. The inhibitory activity is represented as IC_{50} (micrograms/milliliter) except when followed by *, denoting complete neutralization at the indicated concentration in micrograms/milliliter.

Potent Cross-Reactive Inhibitory Activity of m396 and S215.30 in a Mouse Model of SARS-CoV Infection. We used a mouse model of SARS-CoV infection to test whether the potent *in vitro* inhibitory activity correlated with *in vivo* protection from infection. Eight-week-old female BALB/c mice were given m396 at 50 μg or 200 μg per mouse, S230.15 at 200 μg per mouse, or a control antibody specific for Hendra and Nipah viruses at 200 μg per mouse i.p. 24 h before challenge with recombinant SARS-CoVs, Urbani, GD03, or SZ16 (37, 38). Mice that received the control antibody had a mean titer of Urbani, GD03, or SZ16 virus of $10^{8.1}$, $10^{6.4}$, or $10^{7.0}$ at 50% infective dose ($TCID_{50}$) per g of lung tissue, respectively (Fig. 3*a*). Mice that received m396 or S230.15 at 200 μg per mouse were fully protected from challenge with Urbani and GD03 viruses; the protection conferred by m396 from challenge with SZ16 virus was significant but not complete (Fig. 3*a*). The protection conferred by m396 was dose-dependent. The mice receiving 50 μg of m396 were almost completely protected from challenge with SARS-CoV Urbani and less from challenge with GD03 virus. GD03 virus titers in the lungs of mice that received 50 μg of m396 were reduced >1,000-fold compared with titers in mice treated with control antibody ($P = 0.009$). A similar pattern of dose-dependent inhibitory activity against Urbani and GD03 viruses was found *in vitro*

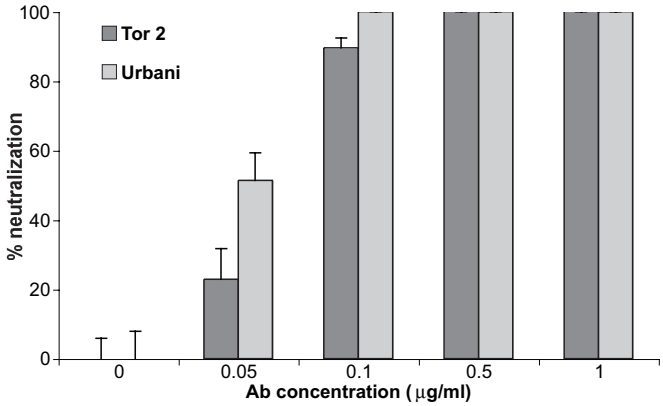

Fig. 2. Potent neutralization of replication-competent virus by m396. Tor2 and Urbani isolates were incubated with IgG1 m396 for 1 h at 37°C before infection. After incubation, the percent neutralization was determined by plaque reduction assay in Vero E6 cells (in duplicate) compared with untreated controls. Bars indicate SE.

(Fig. 1), indicating a correlation between *in vitro* and *in vivo* inhibitory activity.

To find whether the neutralizing activity of the antibodies in mouse serum correlates with their *in vivo* inhibitory activity, we also measured the serum antibody titer by a microneutralization assay. Indeed, the results showed that high serum-neutralizing titer cor-

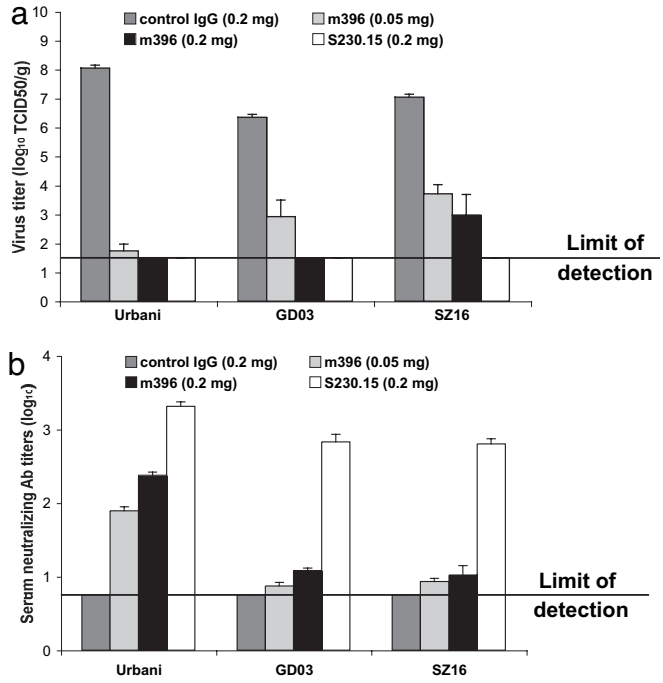

Fig. 3. Potent neutralization of replication-competent recombinant SARS-CoV in mice after antibody administration. (*a*) BALB/c mice, 8 weeks old, were injected i.p with a control monoclonal antibody at 200 μg per mouse; m396 at 50 or 200 μg per mouse; or S230.15 at 200 μg per mouse. Twenty-four hours after antibody administration, mice were bled to evaluate antibody levels in serum and then challenged intranasally with 10^5 $TCID_{50}$ of the respective recombinant SARS-CoV (icUrbani, icGD03, or icSZ16-K479N (SZ16). Virus titers in the lung, determined 2 days after challenge, are expressed as $\log_{10}$ $TCID_{50}$ per g of lung tissue (limit of detection $\leq 10^{1.5}$ $TCID_{50}$ per g of lung tissue). (*b*) Serum-neutralizing antibodies were measured against specific challenge viruses by microneutralization assays. The $\log_{10}$-transformed reciprocal dilution at which 50% neutralization occurred is indicated (limit of detection <8 or $10^{0.9}$). Bars indicate SE.

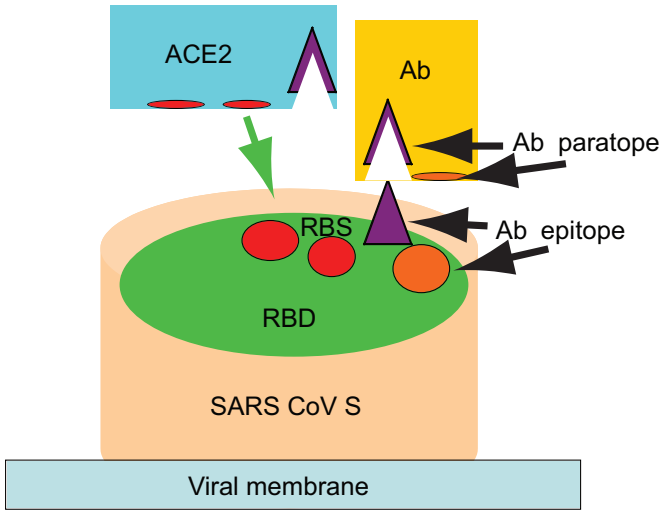

Fig. 4. Schematic representation of the SARS-CoV neutralization mechanism. Competition of the antibody (Ab, Fab m396) with the receptor (ACE2) for binding to the receptor-binding site (RBS) of the RBD of the SARS-CoV S glycoprotein is shown. The protruding portion of the antibody epitope (in violet) is also a major portion of the ACE2 receptor-binding site.

responds to better protection reflected by the low levels of virus in the mouse lungs (compare Fig. 3 *a* and *b*). In addition, mice treated with 200 μg of m396 achieved much higher serum-neutralizing antibody titers to Urbani (1:161 to 1:256) than to GD03 (1:10 to 1:16). The ratio of the two titers ($\approx$10) is the same as the ratio of *in vitro* IC_{50} values for the two isolates (Fig. 1), indicating that the antibody retains about the same neutralizing activity in the serum of animals as in cell culture supernatants. Despite very low levels of serum-neutralizing antibodies the titer of GD03 in the lungs was decreased >1,000-fold. These results suggest that m396 and S230.15 exhibit potent neutralizing activity against isolates from the 2002/2003 and 2003/2004 outbreaks and against a palm civet isolate *in vivo* that correlates with their neutralizing activity *in vitro*.

Competition of m396 and S230.15 with the SARS-CoV Receptor ACE2 for Binding to the RBD as a Mechanism of Their Neutralizing Activity. An analysis of the crystal structure of the RBD·m396 complex predicted that the receptor-binding site on the RBD overlaps the m396 epitope as shown schematically in Fig. 4, and therefore the antibody would compete with the receptor for binding to the virus. To test this prediction and to find the mechanism underlying the neutralizing activity of m396 and S230.15, we used an ELISA to measure ACE2 binding to the RBD in the presence of varying concentrations of the two antibodies. M396 in both formats, Fab and IgG1, competed with ACE2 (SI Fig. 7*B*), as predicted from the crystal structure of the complex. IgG1 was more potent than Fab, in agreement with its higher effective affinity (avidity) to the surface-associated RBD as measured previously by surface plasmon resonance methodology (36). IgG1 S230.15 also competed with ACE2 for binding to the RBD although at somewhat higher concentration (SI Fig. 7*B*). The Fab m396 competed with S230.15 with about the same activity as with IgG m396, indicating a significant overlap of the epitopes of these two antibodies (data not shown). It also competed with mouse monoclonal antibodies that interfere with the ACE2–RBD interactions (conformational epitopes groups III, IV, and VI) (30) (data not shown). These results support the hypothesis that the neutralizing activity of m396 and S230.15 is related to their competition with the receptor ACE2 leading to inhibition of the SARS-CoV interaction with its receptor.

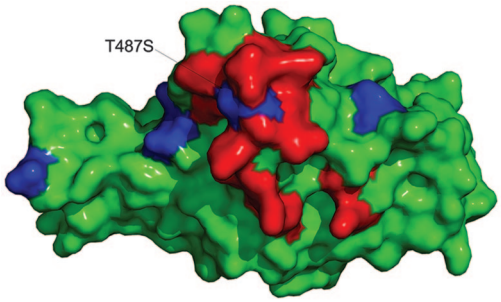

Fig. 5. Amino acid residues that are different in GD03 compared with Urbani (in blue) are located outside the m396 epitope (in red). The antibody contact residues are shown in red on the surface of the RBD crystal structure determined in our previous study (36).

Molecular Mechanisms of the m396 Cross-Reactivity. We used the high-resolution crystal structure of the RBD·m396 complex (36) and site-directed mutagenesis to analyze the molecular mechanisms that determine the high-affinity cross-reactive binding of m396. Guided by the crystal structure, a panel of RBD alanine-scanning mutants was developed to evaluate the relative contribution of m396-contacting residues to binding energy. The mutants were expressed in 293T cells, and their binding to m396 was measured by ELISA. The level of expression of the mutants was about the same, which facilitated the interpretation of the binding data (SI Fig. 7*C*). Considerable (2-fold or more) reduction in binding was observed for RBD with mutated residues R395A, R426A, F483A, Y484A, I489A, Y491A, and Q492A (Fig. 7*C*). When the residue Tyr-491 was replaced with phenylalanine, the reduction was much smaller than when it was replaced with glutamine or alanine, suggesting a role for the benzene ring of the Tyr-491 phenyl group as expected from the crystal structure. The RBD to m396 binding was not decreased or was only weakly decreased when the residues Asp-392, Thr-486, and Thr-487 were mutated to alanine, although according to the crystal structure they contact the antibody. Similarly, replacing Thr-487 with serine decreased binding only weakly. To test the possibility that mutations of RBD residues that do not contact the antibody (noncontact residues) can also affect its binding to the RBD, e.g., by induced conformational changes, we used another panel of RBD mutants and found that mutations of Asp-429, Arg-441, Glu-452, and Asp-454 to alanine also significantly reduced m396 binding (data not shown).

An analysis of the crystal structure of the RBD·m396 complex showed that amino acid changes in RBDs of GD03, SZ3, and SZ16 from the Tor2 (or Urbani) RBD (in blue in Fig. 5) are different from the RBD residues that significantly affect binding to m396 as identified by structure-guided site-directed mutagenesis and described above (in red in Fig. 5). Following this approach, we also analyzed all available sequences of the RBD for SARS-CoV isolates from humans and palm civets. We found a number of amino acid residues that differ from those of the RBD sequence for the prototype Tor2 isolate, which was used in our study to select m396 (Fig. 6). However, none of these residues (except Thr-487, which affects binding weakly) is in contact with m396 according to the crystal structure or affects binding indirectly through noncontact residues (Fig. 6). Thus, mutations of these residues are unlikely to affect significantly the antibody binding to the RBD, which indicates that m396 could neutralize all isolates with available sequences, although some of them with reduced activity (see also Table 1).

Discussion

The major finding of this work is the very high and broad *in vitro* and *in vivo* SARS-CoV-neutralizing activity of the hmAbs m396 and S230.15. Recently, a number of S glycoprotein-specific hmAbs have been identified, and several of them including S3.1 (18), 80R (19), CR3014 (21, 26), scFv B1 (22), and 201 (24) have been extensively characterized. S3.1 prevented the cytopathic effect of the SARS-CoV at 300 ng/ml (18) and inhibited entry of a pseudovirus with S glycoprotein from Urbani isolate with about the same IC_{50} but did not affect entry of a pseudovirus with the GD03 isolate S glycoprotein and even enhanced the entry of virus pseudotyped with the S glycoprotein from the palm civet isolate SZ16 (27). Another antibody, 80R, neutralized 50% of the virus in a microneutralization assay at a concentration as low as 60 ng/ml (19). It also blocked formation of syncytia, although at significantly higher concentration (4 μg/ml). Its epitope overlaps the binding site of the SARS-CoV receptor ACE2, suggesting a possible mechanism of neutralization by preventing the virus attachment to its receptor (19). This antibody was further tested with a pseudovirus assay; it inhibited Tor2 isolate with an IC_{90} of $\approx$2 μg/ml but had no effect on the GD03 isolate (20). The neutralizing activity of this antibody in our cell fusion assay was about 2-fold lower compared with that of m396 (IC_{50} = 1.1 vs. 0.6 μg/ml) for the Tor2 isolate. Another representative antibody, CR3014, protected from the cytopathic effects of two SARS-CoV isolates, FM1 and HKU39849; the concentration for protection from HKU39849 was $\approx$7 μg/ml (21, 26). The scFv B1 neutralized with an IC_{50} of $\approx$4 μg/ml in a pseudovirus assay (22). In a microneutralization assay based on protection for cytopathic effects, the IC_{50} for 201 was $\approx$0.2 μg/ml

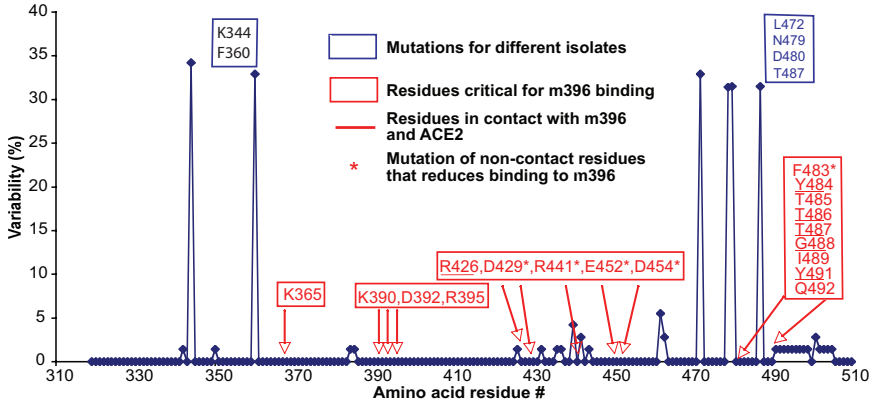

Fig. 6. Analysis of available SARS-CoV sequences and mutagenesis data. M396 is likely to neutralize all isolates with known sequences. Percentage variability is calculated as the ratio of the number of isolates with a specific mutation to the total number of sequences (72) multiplied by 100. Mutations in SARS-CoV RBD sequences are shown in blue. Residues critical for binding to m396 are shown in red. The RBD residues that are in contact with both m396 and ACE2 are underlined. Mutations of noncontact residues that lead to significant decrease of the m396 binding are denoted by an asterisk.

(24). Our results suggest that both m396 and S230.15 exhibit potent inhibitory activity against isolates not only from the first outbreak but also from the second one and from palm civets (Table 1). The *in vitro* neutralizing activity of m396 and S230.15 is about the same or better than that of well characterized SARS-CoV-neutralizing hmAbs for the isolates tested (Table 1). Importantly, m396 and S230.15 did not cause enhancement of virus entry for any isolate tested (data not shown and Table 1) as has been reported for other antibodies tested by the same *in vitro* neutralization assay based on virus pseudotyped with the S glycoproteins of the palm civet isolates SZ3 and SZ16 (27), and mice that had detectable serum neutralizing antibodies had evidence of decreased virus replication in the lung (Fig. 3). We did not see evidence of enhanced virus replication in the lungs in the presence of neutralizing antibodies in the serum that would suggest enhanced disease in the mice.

A major difference between m396 and S230.15, and other hmAbs tested against the GD03 isolate, is the ability of m396 and S230.15 to cross-neutralize isolates from the two SARS outbreaks. One should note that we have recently identified mouse monoclonal antibodies that can also inhibit pseudotyped viruses containing spikes from both outbreaks (39). The availability of the crystal structure of m396 in complex with the RBD allowed analysis of the molecular details of the antibody–RBD interactions. Such analysis showed that the m396 antibody-combining site is a cleft formed by its four complementarity determining regions, namely H1, H2, H3, and L3. The heavy chain alone contributes 65% of the total antibody-combining site surface area with a high structural complementarity to its epitope. The crystal structure shows that this deep pocket could bind to various isolates and accommodate the threonine to serine mutation of residue 487 so it does not significantly affect the RBD–m396 interaction. Site-directed mutagenesis of Thr-487 to either alanine or serine did not significantly change the m396 binding (SI Fig. 7*C*). This finding implies that in the context of this residue, m396 would be potent against SARS-CoV isolates not only from the first outbreak but also from the second one and against isolates from palm civets, which was confirmed by our data. An analysis of all known SARS-CoV isolate sequences together with our mutagenesis data indicate that m396 is likely to neutralize all of them, although differences in neutralization specificity are evident among strains. A note of caution is that there is no guarantee that future isolates will be also sensitive for neutralization by this antibody. The combination of m395 with S230.15 or other potent neutralizing antibodies could decrease the probability for escape mutants with decreased sensitivity to neutralization. Future experiments especially addressing the possibility for escape mutants will show the limits of the antibody cross-reactivity.

Most of the currently known hmAbs with potent neutralizing activity including S3.1, 80R, CR3014, and 201 also significantly reduced virus load in and/or protected mice or ferrets from SARS-CoV infection. It was recently found that mAb201 also exhibits therapeutic efficacy when administered 1 or 2 days after challenge in a hamster model of SARS-CoV infection (25). Thus, it was reasonable to expect that m396 and S230.15 would exhibit similar activity *in vivo*. Indeed our antibodies prevented or attenuated infection of lungs of mice challenged with three different isolates (Urbani, icGOD3, and icSZ16) at 0.2 mg per mouse.

Taken together, our results demonstrate potential antibody-based therapeutics against SARS-CoV which could be used alone or in combination, and they elucidate the molecular mechanisms of their potent and broad neutralizing activity. These human antibodies could be also used for diagnosis and as research reagents in the development of vaccines and inhibitors.

Methods

Antibodies. The production of m396 in different formats was described previously (36). To obtain quantities of IgG1 m396 required for the animal study, we developed a cell line that expresses the antibody at a relatively high level. The identification, expression, and purification of S230.15 were done as described previously (18). The antibody 80R was provided by Wayne Marasco (Harvard Medical School, Boston, MA). The control antibody (against Nipah and Hendra viruses) was isolated and produced by using the same methodology as for m396, which was described previously (40).

Generation, Expression, and Characterization of RBD Mutants. Point mutations were generated at specific residues of the RBD using QuikChange XL site-directed mutagenesis kit (Stratagene, La Jolla, CA) according to the manufacturer's directions. The mutants were expressed and analyzed as described previously (35).

Competition ELISA. Competition among m396, S230.15, and ACE2 for binding to the S protein RBD was measured by using recombinant human ACE2 (R&D Systems, Minneapolis, MN) coated in a coating buffer at 50 ng per well at 4°C overnight, blocked with 3% nonfat milk in PBS, and washed with PBS/Tween (PBST). C-myc-tagged RBD (34) at a final concentration of 2 μg/ml was incubated with a serially diluted Fab and IgG1 m396 and a control IgG1 antibody specific for the Hendra virus G protein, respectively, and the mixtures were then added to ACE2-coated wells in duplicate. After washing, bound c-myc-tagged RBD was detected by using a c-myc tag-specific antibody.

Cell Fusion Inhibition Assay. For assessment of the neutralization activity of the antibodies, a quantitative cell fusion assay based on β-galactosidase (β-gal) as a reporter gene was used as described previously (34). The antibodies were preincubated with 293T cells transfected with the SARS-CoV S glycoprotein gene at room temperature for 10 min, then mixed with 293T cells transfected with ACE2 at 1:1 ratio and incubated at 37°C for 3 h. Cells were then lysed, and the β-gal activity was measured. The antibody concentrations during fusion were used for calculation of the IC_{50} defined as the concentration at which the β-gal activity was reduced by 50%.

Pseudovirus Neutralization Assay. Pseudoviruses containing the S glycoprotein from various virus isolates, and a defective HIV-1 genome that expresses luciferase as a reporter protein, were prepared, and the assays performed as described previously (27, 30, 31).

Infectious Virus Neutralization Assays. Three types of assay were used: plaque reduction, cytopathicity reduction, and microneutralization.

Plaque reduction assay. For this assay, all dilutions were made with Earle's minimum essential medium with 5% heat-inactivated FBS. Challenge virus (SARS-CoV Urbani and Tor2) was diluted to a concentration of 250 pfu/ml, and the antibody preparations ranged from 1.0 to 0.001 μg/ml. The diluted challenge virus was added to each tube of antibody (0.5 ml) in equal volume with gentle mixing. The virus/antibody mixtures were incubated in a 37°C water bath for 1 h and subsequently placed on ice. The amount of infectious virus was quantified by plaque assay in Vero E6 cells. The average number of plaques for two separate wells per sample was determined, and the percent plaque reduction was calculated by using untreated virus as a control. Similar protocol was also used for testing the antibody inhibitory activity against recombinant replication-competent viruses. IC_{50} is defined as the antibody concentration corresponding to 50% neutralization.

Cytopathicity reduction assay. Serial two-fold dilutions of test antibody and control antibody were prepared in duplicate, 50 μl per well, in a 96-well tissue culture plate in Earle's minimum essential medium and supplemented with 2 mM glutamine/500 μg/ml fungizone/100 units/ml penicillin/100 μg/ml streptomycin/10% FBS. An equal volume of SARS-CoV working stock (HKU39849) containing 200 $TCID_{50}$ was added, and the virus/antibody mixture was incubated for 30 min at 37°C in a humidified 5% CO_2 incubator. Vero E6 cell

suspension (100-μl aliquot) at 2×10^5 cells/ml was added to wells of the plate followed by incubation at 37°C in a humidified 5% CO_2 incubator. After 3 days, the plate was observed for cytopathic effect. Neutralization titer was determined from the highest antibody dilution that produced a 100% inhibition of cytopathic effect in both wells.

Microneutralization assays for determination of neutralizing antibody titers. Blood was collected from the tail veins of mice. Serum was heat-inactivated at 56°C for 30 min and assayed for the presence of SARS-CoV-neutralizing antibodies. Two-fold dilutions of sera in L-15 medium (Invitrogen, Carlsbad, CA) were tested in a microneutralization assay for the presence of antibodies that neutralized the infectivity of 100 $TCID_{50}$ of recombinant icUrbani, icGD03, or icSZ16-K479N viruses in Vero cell monolayers as described previously (15).

Construction of icGD03 and icSZ16-K479N Recombinant Viruses Bearing GD03 and SZ16 K479N S Glycoproteins. Information regarding the construction and characterization of icGD03 can be found in Deming *et al.* (41) and Sheahan *et al.* (38). The construction and characterization of icSZ16-K479N (SZ16) were similarly made except that a K479N mutation was introduced (T.S. and R.B., unpublished data). Briefly, the SZ16 spike sequence was inserted into a molecular clone of SARS Urbani. Residue 479 of the spike protein was changed from lysine to asparagine to facilitate human ACE2 binding (42). Recombinant virus was produced as described previously, plaque-purified, and sequence-verified (37).

SARS-CoV Infection in Mice. All experiments with SARS-CoV, including animal studies, were conducted in biosafety level 3 facilities, and all personnel wore personal protective equipment including Tyvek suits and hoods and positive air-purifying respirators. Animal protocols were approved by the Animal Care and Use Committee of the National Institute of Allergy and Infectious Diseases/National Institutes of Health. Eight-week-old female BALB/cAnNTac mice (Taconic, Germantown, NY) were given i.p. injections of 50 μg or 200 μg of m396 or 200 μg of hmAb S230.15 or 200 μg of a control hmAb (0.20 ml total volume, 10 mice per group). One day after administration of mAbs, mice were bled, and sera were assayed for SARS-CoV-specific neutralizing antibodies. After serum collection, mice were lightly anesthetized by isoflurane (USP–Baxter Healthcare, Deerfield, IL) inhalation and challenged intranasally with 10^5 $TCID_{50}$ of recombinant SARS-CoVs icUrbani (37), icSZ16-K479N (T.S. and R.B., unpublished data) or icGD03 (41) in 50 μl total volume. Mice were killed two days after challenge and lungs were harvested for viral titer determination.

Viral Titer Determination. The lungs were homogenized to a final 10% (wt/vol) suspension in Leibovitz's L-15 medium (Invitrogen) with piperacillin (Sigma–Aldrich, St. Louis, MO), gentamicin (Invitrogen), and amphotericin B (Quality Biological, Gaithersburg, MD), which were added to the tissue culture medium at final concentrations of 0.4 mg/liter, 0.1 mg/liter, and 5 mg/liter, respectively. Lung homogenates were clarified by low-speed centrifugation and assayed in serial 10-fold dilutions on Vero cell monolayers as described previously (15). Virus titers are expressed as $TCID_{50}$ per g of lung with a lower limit of detection of $10^{1.5}$ $TCID_{50}$ per g.

Statistical Analyses. The nonparametric Kruskal–Wallis and Mann–Whitney U statistical methods were used for ascertaining the significance of observed differences. Statistical significance was indicated by P values <0.05.

We thank John Owens for useful suggestions. This work was supported in part by the Intramural Research Programs of the National Cancer Institute (NCI) and National Institute of Allergy and Infectious Diseases, National Institutes of Health (NIH), by NCI/NIH Contract N01-CO-12400, and NIH Research Grants AI059443 and AI059136 (to R.B.).

1. Ksiazek TG, Erdman D, Goldsmith CS, Zaki SR, Peret T, Emery S, Tong S, Urbani C, Comer JA, Lim W, *et al.* (2003) *N Engl J Med* 348:1953–1966.
2. Peiris JS, Lai ST, Poon LL, Guan Y, Yam LY, Lim W, Nicholls J, Yee WK, Yan WW, Cheung MT, *et al.* (2003) *Lancet* 361:1319–1325.
3. Drosten C, Gunther S, Preiser W, van der Werf S, Brodt HR, Becker S, Rabenau H, Panning M, Kolesnikova L, Fouchier RA, *et al.* (2003) *N Engl J Med* 348:1967–1976.
4. Holmes KV (2003) *N Engl J Med* 348:1948–1951.
5. Liang G, Chen Q, Xu J, Liu Y, Lim W, Peiris JS, Anderson LJ, Ruan L, Li H, Kan B, *et al.* (2004) *Emerg Infect Dis* 10:1774–1781.
6. Chinese SARS Molecular Epidemiology Consortium (2004) *Science* 303:1666–1669.
7. Song HD, Tu CC, Zhang GW, Wang SY, Zheng K, Lei LC, Chen QX, Gao YW, Zhou HQ, Xiang H, *et al.* (2005) *Proc Natl Acad Sci USA* 102:2430–2435.
8. Li W, Wong SK, Li F, Kuhn JH, Huang IC, Choe H, Farzan M (2006) *J Virol* 80:4211–4219.
9. Hsueh PR, Huang LM, Chen PJ, Kao CL, Yang PC (2004) *Clin Microbiol Infect* 10:1062–1066.
10. Nie Y, Wang G, Shi X, Zhang H, Qiu Y, He Z, Wang W, Lian G, Yin X, Du L, *et al.* (2004) *J Infect Dis* 190:1119–1126.
11. Shi Y, Wan Z, Li L, Li P, Li C, Ma Q, Cao C (2004) *J Clin Virol* 31:66–68.
12. Han DP, Kim HG, Kim YB, Poon LL, Cho MW (2004) *Virology* 326:140–149.
13. Guo JP, Petric M, Campbell W, McGeer PL (2004) *Virology* 324:251–256.
14. Hofmann H, Hattermann K, Marzi A, Gramberg T, Geier M, Krumbiegel M, Kuate S, Uberla K, Niedrig M, Pohlmann S (2004) *J Virol* 78:6134–6142.
15. Subbarao K, McAuliffe J, Vogel L, Fahle G, Fischer S, Tatti K, Packard M, Shieh WJ, Zaki S, Murphy B (2004) *J Virol* 78:3572–3577.
16. Roberts A, Vogel L, Guarner J, Hayes N, Murphy B, Zaki S, Subbarao K (2005) *J Virol* 79:503–511.
17. McAuliffe J, Vogel L, Roberts A, Fahle G, Fischer S, Shieh WJ, Butler E, Zaki S, St Claire M, Murphy B, *et al.* (2004) *Virology* 330:8–15.
18. Traggiai E, Becker S, Subbarao K, Kolesnikova L, Uematsu Y, Gismondo MR, Murphy BR, Rappuoli R, Lanzavecchia A (2004) *Nat Med* 10:871–875.
19. Sui J, Li W, Murakami A, Tamin A, Matthews LJ, Wong SK, Moore MJ, Tallarico AS, Olurinde M, Choe H, *et al.* (2004) *Proc Natl Acad Sci USA* 101:2536–2541.
20. Sui J, Li W, Roberts A, Matthews LJ, Murakami A, Vogel L, Wong SK, Subbarao K, Farzan M, Marasco WA (2005) *J Virol* 79:5900–5906.
21. van den Brink EN, ter Meulen J, Cox F, Jongeneelen MA, Thijsse A, Throsby M, Marissen WE, Rood PM, Bakker AB, Gelderblom HR, *et al.* (2005) *J Virol* 79:1635–1644.
22. Duan J, Yan X, Guo X, Cao W, Han W, Qi C, Feng J, Yang D, Gao G, Jin G (2005) *Biochem Biophys Res Commun* 333:186–193.
23. Zhang MY, Choudhry V, Xiao X, Dimitrov DS (2005) *Curr Opin Mol Ther* 7:151–156.
24. Greenough TC, Babcock GJ, Roberts A, Hernandez HJ, Thomas WD, Jr, Coccia JA, Graziano RF, Srinivasan M, Lowy I, Finberg RW, *et al.* (2005) *J Infect Dis* 191:507–514.
25. Roberts A, Thomas WD, Guarner J, Lamirande EW, Babcock GJ, Greenough TC, Vogel L, Hayes N, Sullivan JL, Zaki S, *et al.* (2006) *J Infect Dis* 193:685–692.
26. ter Meulen J, Bakker AB, van den Brink EN, Weverling GJ, Martina BE, Haagmans BL, Kuiken T, de Kruif J, Preiser W, Spaan W, *et al.* (2004) *Lancet* 363:2139–2141.
27. Yang ZY, Werner HC, Kong WP, Leung K, Traggiai E, Lanzavecchia A, Nabel GJ (2005) *Proc Natl Acad Sci USA* 102:797–801.
28. He Y, Zhou Y, Liu S, Kou Z, Li W, Farzan M, Jiang S (2004) *Biochem Biophys Res Commun* 324:773–781.
29. Jiang S, He Y, Liu S (2005) *Emerg Infect Dis* 11:1016–1020.
30. He Y, Lu H, Siddiqui P, Zhou Y, Jiang S (2005) *J Immunol* 174:4908–4915.
31. He Y, Zhu Q, Liu S, Zhou Y, Yang B, Li J, Jiang S (2005) *Virology* 334:74–82.
32. Chen Z, Zhang L, Qin C, Ba L, Yi CE, Zhang F, Wei Q, He T, Yu W, Yu J, *et al.* (2005) *J Virol* 79:2678–2688.
33. Yi CE, Ba L, Zhang L, Ho DD, Chen Z (2005) *J Virol* 79:11638–11646.
34. Xiao X, Chakraborti S, Dimitrov AS, Gramatikoff K, Dimitrov DS (2003) *Biochem Biophys Res Commun* 312:1159–1164.
35. Chakraborti S, Prabakaran P, Xiao X, Dimitrov DS (2005) *Virol J* 2:73.
36. Prabakaran P, Gan J, Feng Y, Zhu Z, Choudhry V, Xiao X, Ji X, Dimitrov DS (2006) *J Biol Chem* 281:15829–15836.
37. Yount B, Roberts RS, Sims AC, Deming D, Frieman MB, Sparks J, Denison MR, Davis N, Baric RS (2005) *J Virol* 79:14909–14922.
38. Sheahan T, Deming D, Donaldson E, Pickles R, Baric R (2006) *Adv Exp Med Biol* 581:547–550.
39. He Y, Li J, Li W, Lustigman S, Farzan M, Jiang S (2006) *J Immunol* 176:6085–6092.
40. Zhu Z, Dimitrov AS, Bossart KN, Crameri G, Bishop KA, Choudhry V, Mungall BA, Feng YR, Choudhary A, Zhang MY, *et al.* (2006) *J Virol* 80:891–899.
41. Deming D, Sheahan T, Heise M, Yount B, Davis N, Sims A, Suthar M, Harkema J, Whitmore A, Pickles R, *et al.* (2006) *PLoS Med* 3:e525.
42. Li F, Li W, Farzan M, Harrison SC (2005) *Science* 309:1864–1868.